Cumulative distribution of the stretching and twisting of vortical structures in isotropic turbulence.

Daniela Tordella♮* and Luca Sitzia♯
♮ *Dipartimento di Ingegneria Aeronautica e Spaziale, Politecnico di Torino, Corso Duca degli Abruzzi 24, 10129 Torino, Italy*
♯ *Dottorato in Statistica e Matematica Applicata, Scuola di Dottorato "V.Pareto" - Universita' di Torino, via Real Collegio 30, 10024 Moncalieri (To), Italy*
(Dated: May 5, 2010)

Using a Navier-Stokes isotropic turbulent field numerically simulated in the box with a discretization of 1024^3 (Biferale L. et al. *Physics of Fluids*, **17**(2), 021701/1-4 (2005)), we show that there is zero probability of having a stretching-twisting larger than twice the local enstrophy. It can be observed that, in the unfiltered isotropic field, the probability of the ratio $(|\boldsymbol{\omega}\cdot\nabla\mathbf{U}|/|\boldsymbol{\omega}|^2)$ being higher than a given threshold is higher than that of the fields where the large scales were filtered out. At the same time, it is lower than that of the fields were the inertial and small scales were filtered out. This is basically due to the suppression of compact structures in the differently filtered ranges. The partial removal of the background of filaments and sheets does not have a first order effect on these statistics. The stretching and twisting components are nonskewed but show high kurtosis, 4.6 and 5.28, respectively. These results agree with some aspects observed in recent experimental analyses of the properties of the isotropic fluctuation vorticity field and of the stretching and tilting of turbulent material lines.

PACS numbers: 47.27.Ak, 47.27.eb, 47.27.Gs, 47.32.C-

I. INTRODUCTION

The formation of spatial and temporal internal scales can in part be associated to the stretching and twisting of vortical structures. Many aspects of the behavior of turbulent fields have been associated to this phenomenon: the onset of instability, vorticity intensification or damping, the three-dimensionalization of the flow field [1–3]. In the standard picture of turbulence, the energy cascade to smaller scales is interpreted in terms of the stretching of vortices due to the interaction with similar eddy sizes [4]. Although the important physical role of these inertial phenomena is recognized, the literature does not often report statistical information on quantities such as the magnitude or the components of $\boldsymbol{\omega}\cdot\nabla\mathbf{U}$. Statistics concerning other gradient quantities, such as the strain rate or the rate-of-rotation tensors, are more common. Statistics on the skewness and flatness factors of the velocity derivative have often been considered over the last 20 years in a number of laboratory and numerical studies that show how these quantities increase monotonically the with Reynolds number, see e.g. [5] and the review by Sreenivasan and Antonia (1997)[6]. However, a few examples can also be cited as far as direct results concerning stretching-twisting statistics are concerned. In the case of turbulent wall flows, laboratory measurements of both the mean and the r.m.s. of fluctuations of the stretching components across the two-dimensional boundary layer have been reported by Andreapoulos and Honkan (2001) [7]. In this study, the normalized r.m.s values of the stretching components are very significant throughout the boundary layer and reach values that are one order of magnitude larger than the mean span-wise component (the only significant mean component, however and only in the near wall region). The observed values for the r.m.s. of the stretching range from 0.04, close to the wall, to about 0.004 in the outer part. Other laboratory statistical information on the stretching of field lines can be found in [8, 9]. In the first study, probability density functions of the logarithm of the local stretching in N cycles were obtained for several two-dimensional time-periodic confined flows exhibiting chaotic advection. The stretching fields were observed to be highly correlated in space when N is large, and the probability distributions were observed to be similar for different flows. In the second study, the stretching and tilting of material lines in quasihomogeneus turbulence ($Re_\lambda = 50$) was considered. In particular, the tensor of the velocity derivatives along particle trajectories was measured by means of 3D particle tracking velocimetry. It was observed that a statistically high level of vorticity reduces the stretching rate and alters the orientation of the material lines with regard to the extensional eigenvector of the rate of the strain tensor. On the contrary, when the vorticity magnitude is low, the strain rate contributes to a great extent to both tilting and stretching. Using data from highly resolved direct numerical simulations, Hamlington et al. [10] have given a direct assessment of vorticity alignment with the most extensional eigenvector of the *nonlocal* strain rate together with some evidence of

*Electronic address: daniela.tordella@polito.it

the tendency toward a smaller vorticity stretching ratio (backgroung to local) for a large vorticity magnitude in incompressible homogeneous turbulence.

In the present work, for the case of isotropic turbulence ($Re_\lambda = 280$, [11]), we consider statistics related to the intensity of the stretching-tilting of vortical filaments, sheets and blobs with reference to their vorticity magnitude.

II. THE NORMALIZED STRETCHING-TWISTING FUNCTION

With reference to the phenomena described by the inertial nonlinear nonconvective part of the vorticity transport equation, let us introduce a local measure of the process of three-dimensional inner scales formation

$$f(\mathbf{x},t) = \frac{|(\boldsymbol{\omega} - \langle\boldsymbol{\omega}\rangle)\cdot\nabla(\mathbf{U} - \langle\mathbf{U}\rangle)|}{|(\boldsymbol{\omega} - \langle\boldsymbol{\omega}\rangle)|^2}(\mathbf{x}) \qquad (1)$$

where $\mathbf{U} = \langle\mathbf{U}\rangle + \mathbf{u}$ is the velocity field, $\boldsymbol{\omega} = \nabla\times\mathbf{U}$ is the vorticity vector and the brackets $\langle\cdot\rangle$ represent statistically averaged quantities. According to this definition, f depends on the local instantaneous velocity and vorticity fields. Since we only wish to refer to the action of the turbulent fluctuation field, the contributions of the mean velocity and vorticity flow have been subtracted. In isotropic turbulence, $\langle\mathbf{U}\rangle$ and $\langle\boldsymbol{\omega}\rangle$ are zero, thus definition (1) reduces to

$$f(\mathbf{x}) = \frac{|\boldsymbol{\omega}\cdot\nabla\mathbf{U}|}{|\boldsymbol{\omega}|^2}(\mathbf{x}). \qquad (2)$$

The numerator, $|\boldsymbol{\omega}\cdot\nabla\mathbf{U}|$, the so called stretching-twisting (or tilting) term of the vorticity equation, is zero in two-dimensional flows. In 3 D fields, it is responsible for the transfer of the kinetic energy from larger to smaller scales (positive or extensional stretching) and viceversa (negative or compressional stretching) and for the three-dimensionalization of the vorticity field. The denominator in (2) is the magnitude of the vorticity, which, leaving aside a factor 1/2, is usually referred to as enstrophy, the only invariant of the rate-of-rotation tensor different from zero.

Function f was evaluated over a fully resolved homogeneous isotropic incompressible steady in the mean turbulence in order to look for the typical range of values of $f(\mathbf{x})$ and to relate them to the behavior of the various turbulence scales present in an isotropic field. The database consists of 1024^3 resolution grid point Direct Numerical Simulation (DNS) of an isotropic Navier-Stokes forced field, at Reynolds $Re_\lambda = 280$ [11]. Each instant in the simulation is statistically equivalent, and provides a statistical set of a little more than 10^9 elements. We considered the statistics that were obtained averaging over three time instants. The field has been slightly modified

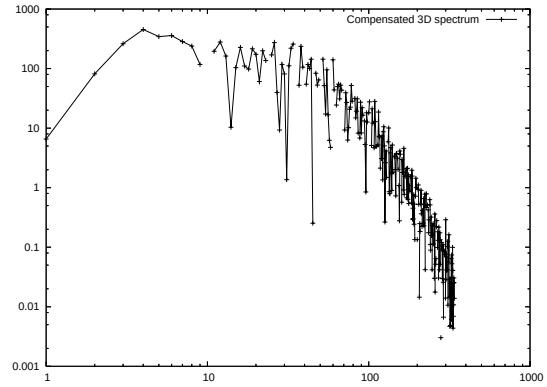

FIG. 1: Compensated 3D energy spectrum

in order to filter out the instantaneous effects of the forcing, in other words, a turbulent kinetic energy inhomogeneity of about 20% (in the spatial coordinate system). As this bias was generated by the energy supply at the large scale range, the two largest scales have been filtered out. The resolved part of the energy spectrum extends up to $k \sim 330$. The inertial range extends from $k \sim 10$ to $k \sim 70$, see the compensated version of the 3D spectrum in figure 1. The higher wave-numbers, which are affected by the aliasing error, are not shown.

The range of values attained by $f(\mathbf{x})$ is wide. Values as high as a few hundreds were observed at a few spatial points. In order to read the typical values of $f(\mathbf{x})$, we study its *survival function*. By denoting $F(s) = P(f(\mathbf{x}) \le s)$ the cumulative distribution function (cdf) of $f(\mathbf{x})$, the survival function is defined as the complement to 1 of the cdf,

$$S(s) = P(f(x) > s) = 1 - F(s). \qquad (3)$$

For each threshold s, $S(s)$ describes the *probability that* $f(\mathbf{x})$ *takes greater values than* s.

It has been found that, when $f(\mathbf{x})$ is evaluated on the reference turbulent field, the probability that $f(\mathbf{x}) > 2$ is almost zero, see figure 2. Thus, $f(\mathbf{x}) = 2$ can be considered the maximum statistical value that $f(\mathbf{x})$ can reach when the turbulence is simulated with a fine grain.

III. PROPERTIES OF THE SURVIVAL FUNCTION OF THE NORMALIZED STRETCHING-TWISTING: ANALYSIS ON FILTERED FIELDS

The application of filters to the velocity field, by means of suitable convolutions, in principle allows the behavior of the function $f(x)$ to be studied in relation to the different scale ranges of the turbulence. This analysis is carried out using two filters, a high pass and a band pass filter.

The first filter is a cut-off filter, which we refer to as *cross filter* and which allows the contribution of the struc-

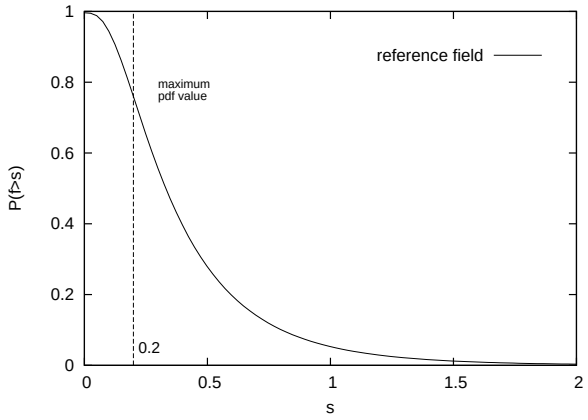

FIG. 2: Survival probability of the normalized stretching-twisting function in a fully resolved isotropic 3D turbulent field ($P(f(\mathbf{x}) \geq s)$. Unfiltered velocity field.

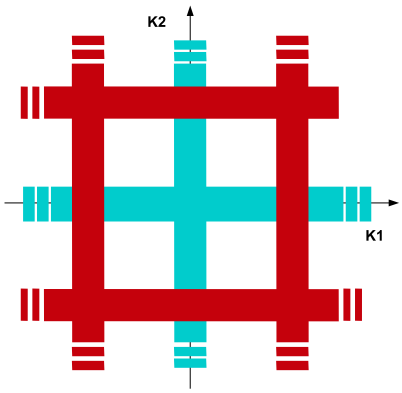

FIG. 3: Scheme of the filter CROSS that can be used as i) a high-pass filter: the wave-numbers under a certain threshold are partially removed, see (4) (region in blue in the k_1, k_2 wavenumber plane), ii) both a band-pass and a low-pass filter: the wave-numbers inside a range, or above a certain threshold, are cut, see (5-7) (region in red).

tures that are characterized by at least one *large dimension* to be removed. From the Fourier point of view, this means that the structures whose wave-vector has at least one small component are filtered out. See, in figure 3, a graphical scheme of the filtering in the wave number plane k_1, k_2 (part in blue). We are thus using a sort of high-pass filter, which affects all wave-numbers that, along any possible direction, have at least one component under a certain threshold. Given the threshold k_{MAX}, the filter reduces the contribution of the modes with wave number components

$$k_1 < k_{MAX} \quad \text{or} \quad k_2 < k_{MAX} \quad \text{or} \; k_3 < k_{MAX}.$$

The representation of this high-pass filter, g_{hp}, can be given by a function of the kind [12]

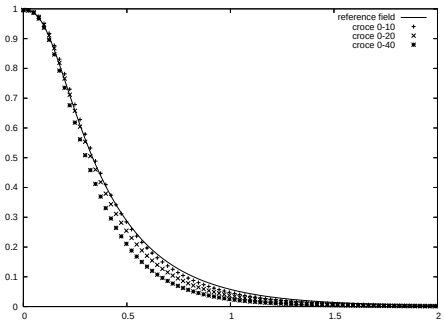

FIG. 4: Survival probability of the normalized stretching-twisting function in a high pass filtered isotropic turbulent field; high-pass filtering

$$g_{hp}(\underline{k}) \; = \; \prod_i \phi(k_i), \; \phi(k_i) = \frac{1}{1 + e^{-(k_i - k_{MAX})}} \qquad (4)$$

Since function g_{hp} filters any wavenumber that has at least one component lower than the threshold k_{MAX}, it reduces the kinetic energy of the filamentous (one component lower than k_{MAX}), layered (two components lower than k_{MAX}) and blobby (three components lower than k_{MAX}) structures. This filter is efficient in reducing the integral scale of the turbulence [12].

By varying the value of the threshold, k_{MAX}, it is possible to consider different scale ranges. The ranges $0-10, 0-20, 0-40$ are compared in fig.4. The first filtering affects the energy-containing range, while the other two also include a part of the inertial range, see figure 1. The plots in this figure have coherent behavior. The survival function S for the $0-10$ filtering is slightly below the values of the distribution of the unfiltered turbulence. This trend is confirmed by the other two filterings, and the reduction grows as the threshold k_{MAX} increases. The high-pass filter has the effect of *decreasing* the statistical values taken by $f(x)$ in the domain. The wider the filtered range, the higher the effect on f.

It is possible to say that when we reduce the weight of the large-scale structures (layers, filaments or blobs), the local stretching-twisting process undergoes a general *decrease* with respect to the vorticity intensity. On average, the values of $f(x)$ go down; and the wider the range affected, the lower the probability value becomes. This suggests that the large scales contribute more to the stretching-twisting (the numerator of f) than to the fluctuation vorticity magnitude (the denominator of f). It should be noted that, leaving aside the issue related to the alignement of the vorticity vector with the eigenvectors of the strain rate tensor, a point that has not been considered in the present study, this trend is consistent with the results in [9 - 10]. This consistency also includes the results relevant to the fluctuation stretching

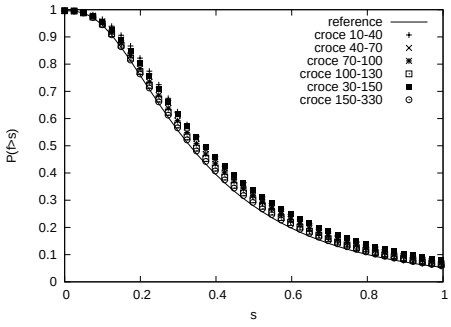

FIG. 5: Probability of the normalized stretching-twisting function in a band pass filtered (in the inertial range) isotropic turbulent field of being higher than a threshold s. Control function $1 - F(x)$, band pass filtering.

and vorticity magnitude behavior in the boundary layer turbulence, see fig.s 6 and 9 in [7]. For the large range $0 - 40$, a decrease of 30% in the cumulative probability is observed for a stretching-twisting of about one half of the local vorticity. The decrease goes up to 80% for a stretching-twisting of the same magnitude of the vorticity, see figure 4.

Let us now consider the behavior of $f(x)$ when the inertial and dissipative ranges are affected by the filtering, namely a band pass filtering. In case, the band width can be extended to obtain a low pass filtering.

This filter can be obtained by reducing the contribution of a variable band (see fig.3, the part in red)

$$k_{MIN} < k_1 < k_{MAX} \quad \text{or} \quad k_{MIN} < k_2 < k_{MAX} \text{ or } k_{MIN} < k_3 < k_{MAX}.$$

This yields the filter function g_{bp}

$$g_{bp}(\underline{k}) = \prod_i \overline{\phi}(k_i; k_{MIN}, k_{MAX}), \tag{5}$$

$$\phi(k_i; k_0) = \frac{1}{1 + e^{-(k_i - k_0)}}, \tag{6}$$

$$\overline{\phi}(k_i; k_{MIN}, k_{MAX}) = [1 - \phi(k_i; k_{MIN})] + \phi(k_i; k_{MAX}) \tag{7}$$

The effects of the application of this band-pass filter on the probability $P(f(\mathbf{x}) \geq s)$ are shown in fig.5.

Let us now consider the inertial range in an *extended way*, which includes the $-\frac{5}{3}$ range plus all the scales which are not yet dissipative. The different bands are $10 - 40$, large scale inertial filtering, $40 - 70$ intermediate scale inertial filtering, $70 - 100$ small scale inertial filtering, $100-130$ near dissipative, $30-150$ intermediate-inertial/small scale filtering, $150 - 330$ dissipative. Once again all the filtered ranges induce the same effects: for $s < 1/2$, a slight *increase* in the survival probability; For small values of s, the most effective filtering (i.e. the ones which percentually produce the strongest increase) are the $10 - 40, 40 - 70$ ranges, while, for higher statistically relevant values, $0.5 < s < 2$, the most effective result is obtained filtering over the whole inertial range, $30 < k < 150$. An increase of about 60% is observed for $s = 1$ and of more than 100% for $s = 1.5$

This highlights the fact that the structures of the inertial range contribute more to the intensity of the vorticity field than to stretching and twisting. The general trend is almost inverted with respect to the case of the high pass filtered turbulence (compare the 0-40 and 10-40 results in figures 4 and 5, respectively) and this can be confirmed, with slight differences, as long as we enlarge the amplitude of the filtering band to get closer to the dissipative range.

Finally, moving toward the dissipative range ($150 < k < 330$), the band pass filter becomes a sort of low-pass filter. By filtering these wave numbers, the obtained effect is minimum, although we have removed the contribution of more or less the highest 200 wave-numbers (see figure.5).

At this point, let us consider the dual nature of the filaments and sheets, as regards their inclusion in the categories of the small and large scales. A filament which is filtered out by the filter g_{hp} because it has a small wave number (the axial wave number component), will have two large wave number components (the ones normal to the axis). Because of these wave components, it will also be filtered out by the filter g_{bp}. A similar situation also hold for the sheets. Thus filaments and sheets are always filtered. The filtering, either the high pass, low pass or band-pass one, always removes the same structures. What makes the difference are the compact structures (the blobs), which non ambiguously belong either to the large scale range or to the intermediate-small scale range. The different behavior shown in fig.s 4 and 5 is therefore mainly due to the blobs contributions, and, since the variation in the cumulative distributions is opposite and almost of the same magnitude, it is possible to deduce that the partial removal of the background filaments and sheets, which is always done regardless of the filter typology (high pass, band pass, low pass,..), is neutral as regards the statistics. In other words, the filament and sheet partial removal does not produce a statistical modification of the stretching intensity values with respect to the vorticity magnitude.

IV. FURTHER CONSIDERATIONS

Up to now, we have considered the influence that different coherent structures have on the statistical properties of the scalar function $f(\mathbf{u}) = \frac{|\boldsymbol{\omega} \cdot \nabla \mathbf{u}|}{|\boldsymbol{\omega}|^2}$. However, stretching-twisting is a phenomenon of an intrinsic vectorial nature. We have thus also considered the statistical properties of $\frac{\boldsymbol{\omega} \cdot \nabla \mathbf{u}}{|\boldsymbol{\omega}|^2}$. The pdf of the components (which are all alike, since the field is statistically homogeneous and isotropic) of the vector $\frac{\boldsymbol{\omega} \cdot \nabla u}{|\boldsymbol{\omega}|^2}$ is shown in figure 6. Symmetry with the vertical axis is expected be-

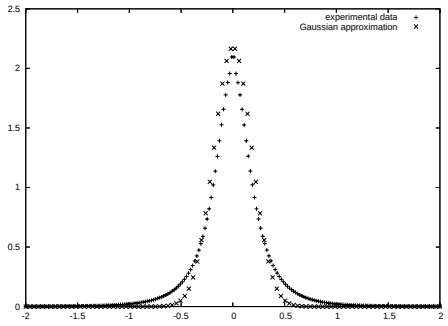

FIG. 6: Pdf of $\frac{\boldsymbol{\omega}\cdot\nabla u}{|\boldsymbol{\omega}|^2}$, and comparison with the Gaussian model

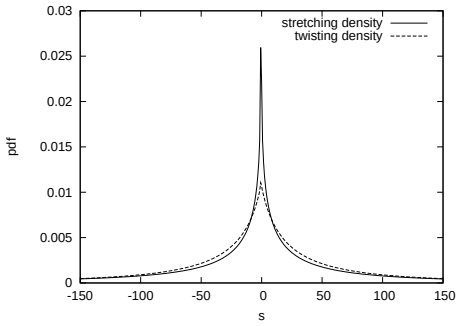

FIG. 7: Distribution of the stretching and twisting components

cause of isotropy; the skewness is in fact approximately 10^{-2}, which is not meaningfully far from zero. However, the distribution cannot be approximated with a *Gaussian* function. In fact, the actual kurtosis is approximately 55, which is very far from the Gaussian value of 3.

Finally, we show the distribution for the unfiltered turbulence of the two components involved in the basic scale differentiation process: – the stretching (positive, extensional, scale reducing, or the negative, compressional, scale enlarging one) and – the three-dimensionalization (vortex twisting). The *stretching* terms can be isolated in the vector

$$(\boldsymbol{\omega}_x\frac{\partial u}{\partial x},\boldsymbol{\omega}_y\frac{\partial u}{\partial y},\boldsymbol{\omega}_z\frac{\partial u}{\partial z}) \tag{8}$$

while the *twisting* phenomenon is governed by the term

$$(\boldsymbol{\omega}_y\frac{\partial v}{\partial x}+\boldsymbol{\omega}_z\frac{\partial w}{\partial x},\boldsymbol{\omega}_x\frac{\partial u}{\partial y}+\boldsymbol{\omega}_z\frac{\partial w}{\partial y},\boldsymbol{\omega}_x\frac{\partial u}{\partial z}+\boldsymbol{\omega}_y\frac{\partial v}{\partial z}) \tag{9}$$

where, as usual, (u,v,w) is the velocity field and $\boldsymbol{\omega}=(\boldsymbol{\omega}_x,\boldsymbol{\omega}_y,\boldsymbol{\omega}_z)$ is the vorticity vector in a Cartesian reference system. The pdf of these quantities are shown in figure 7. We have only shown one component of each vector (the z-component), which here is not normalized by $|\boldsymbol{\omega}|^2$. The other two are analogous since the turbulence is isotropic. The skewness is negligible and the kurtosis is equal to 4.6 and 5.28, respectively. It is interesting to observe that the mean value of the stretching is almost twice as probable as that of the twisting and that the kurtosis of the twisting is higher than that of the stretching, which indicates a higher intermittency of the three-dimensionalization process.

V. CONCLUSIONS

In short, we have collected a set of statistical information about the stretching and twisting of vortical structures, $f(\mathbf{x})=\frac{|\boldsymbol{\omega}\cdot\nabla\mathbf{U}|}{|\boldsymbol{\omega}|^2}(\mathbf{x})$, in isotropic turbulence. A first result is that there is zero probability of having a larger stretching/twisting of intensity than the double of the square of the vorticity magnitude. Then, if compact structures (blobs) in the inertial range are filtered out, it can be seen that the probability of having higher f than a given threshold s increases by 20% at $s=0.5$, and by 60-70% at $s=1.0$. If larger blobs are instead filtered, an opposite situation occurs. The unfiltered field is thus a separatrix for the cumulative probability function. This behavior - high fluctuation vorticity magnitude $\rightarrow$ low stretching, and viceversa - agrees with general aspects highlighted by different laboratory and numerical analysis [8 - 10], also in near wall turbulent flow configurations [7]. The present observations must be associated to the non discriminating effect of filtering on filaments and sheets, which is due to their specific nature that cannot be reconciled inside either a category of small or large scales. It has also been shown that a high intermittency is associated to f, whose kurtosis is as high as 55, and that the non normalized twisting component is more intermittent than the stretching component. In other words, the tilting of field lines is subject to more intense fluctuations than the process of change of scale (which is relevant to both the positive (elongation) and negative (compression) stretching. The three-dimensionalization process is therefore less smooth than the nonlinear scale variation.

Lastly, it is interesting to observe that box filtering small scales modifies the stretching statistics to a great extent. A field filtered in such a way shows a finite probability of having a larger stretching/twisting larger than twice the enstrophy [13, 14]. In the context of the Large Eddy Simulation methodology, where this filtering is commonly used, it is possible to deduce that, when a fluctuating field shows such a feature, the field is unresolved. As a consequence, it is possible to build a criterion that locates the regions of the field where the inclusion of a subgrid term in the governing equations is advisable.

VI. ACKNOWLEDGMENTS

We are grateful to Professor James J. Riley for many fruitful discussions. This work was carried out in cooper-

ation with the International Collaboration for Turbulence Research.

[1] A.S. Monin and A.M. Yaglom *Statistical Fluid Mechanics.* Vol.s 1-2, The MIT Press, Cambridge, Massachusetts, and London, England., (1971, 1975).

[2] H. Tennekes and J.L. Lumley *A first course in turbulence*, The MIT Press, Cambridge, Massachusetts, and London, England., (1972).

[3] S.B. Pope, *Turbulent flows*, Cambridge University Press, (2000).

[4] U. Frisch, *Turbulence - The legacy of A.N. Kolmogorov*, Cambridge University Press, (1995).

[5] A. Tsinober, E. Kit, T. Dracos, J.Fluid Mech., **242**, 169 (1992).

[6] K. R. Sreenivasan and R. A. Antonia, Annu. Rev. Fluid Mech. **29**, 435 (1997).

[7] Y. Andreapoulos and A. Honkan, J. Fluid Mech., **439**, 131 (2001).

[8] P.E. Arratia and J.P. Gollub, J. Stat. Phys., **121**, Nos. 516, 805 (2005). J. Fluid Mech., **439**, 131 (2001).

[9] M. Guala, A. Liberzon, B. Luthi, W.Kinzelbach, and A. Tsinober, Phyis. Review E, **73**, 036303 (2006).

[10] P.E. Hamlington, J. Schumacher and W.J.A. Dahm Phys. of Fluids, **20**, 111703 (2008).

[11] L. Biferale, G. Boffetta, A. Celani, A. Lanotte, F. Toschi, Phys. of Fluids. **17**(2), 021701/1-4 (2005).

[12] D. Tordella and M. Iovieno, J. Fluid Mech. **549**, 441 (2006).

[13] D. Tordella, M. Iovieno, S. Massaglia, Comput. Phys. Commun., **176**, 539 (2007).

[14] D. Tordella, M. Iovieno, S. Massaglia, Comput. Physics Commun. **178**, 883 (2008).